Journal of Membrane Science 360 (2010) 217–225

Contents lists available at ScienceDirect

Journal of Membrane Science

journal homepage: www.elsevier.com/locate/memsci

An analytical solution for heat mass transfer in a hollow fiber membrane based air-to-air heat mass exchanger

Li-Zhi Zhang*

Key Laboratory of Enhanced Heat Transfer and Energy Conservation of Education Ministry, School of Chemistry and Chemical Engineering, South China University of Technology, Guangzhou 510640, China

ARTICLE INFO

Article history:
Received 19 February 2010
Received in revised form 30 April 2010
Accepted 3 May 2010
Available online 8 May 2010

Keywords:
Hollow fiber membranes
Air-to-air heat exchanger
Heat transfer
Mass transfer

ABSTRACT

Hollow fiber membrane modules have been employed for heat and moisture recovery from ventilation air. There are several benefits with this structure. The contact area is large. The resulting NTU (Number of Transfer Units) is high, which implicates a high performance. In this research, the governing equations for heat and moisture transfer in the module are proposed. The equations are then normalized with dimensionless parameters. Following this step, an analytical solution is obtained for the dimensionless differential governing equations. With the developed analytical solution, the sensible and latent heat exchange effectiveness could be estimated by simple algebraic calculations. This provides a convenient yet accurate tool for component design and system optimization. Experiments are conducted to validate the model. Effects of varying operating conditions on module performances are discussed. The study provides a tool for hollow fiber module optimization with simple correlations.

1. Introduction

Indoor air quality has gained much attention recently [1–6]. Sufficient fresh air supply by ventilation is necessary for occupant's health. The obvious way to get more fresh air is to open a window. After all, that is one reason to put windows in buildings in the first place. However opening a window subverts the reason that the building is insulated in the first place. Sensible and latent load accompanying the incoming fresh air are heavy. In hot and humid regions like Guangdong, conditioning fresh air represents 1/3 of the total load for air conditioning. It is thus significant to recover the cool and dryness from the exhaust air stream in summer [7–13].

Heat mass exchangers (total heat exchangers, or the so-called energy recovery ventilators) [7–13] could save a large fraction of energy that is used for cooling and dehumidifying the fresh air. With heat mass exchangers, the efficiency of an existing HVAC system can also be improved. The reason is that traditionally the fresh air is dehumidified by cooling coil condensation and subsequent reheating processes, which are very energy intensive. On the other hand, this part of energy can be saved if heat mass exchangers are installed to reduce the dehumidification load. The cooling coil condensation can be prevented. In addition, the heat mass exchangers are helpful for the prevention of epidemic respiratory diseases like SARS, H1N1, and bird flu.

Permselective membranes have been employed to realize this goal. Parallel-plates type membrane heat mass exchangers have been studied extensively [7,8]. The structure is simple. However, the packing density is low. As a consequence, the heat and moisture exchange effectiveness is quite limited.

Hollow fiber membranes are a promising alternative. In this concept, a bundle of hollow fiber membranes is packed in a shell to form a module. The structure is like a shell-and-tube heat exchanger [9]. The fresh air and the exhaust airflow in the tube side and shell side respectively. They exchange heat and moisture through the membrane wall. The membrane-made fibers are in a diameter of 1–3 mm, so the packing density is rather high. The contact area between the two air streams can be as high as 1000 m^2/m^3. As a result, the heat and moisture exchange effectiveness can be high enough to attract commercial interests.

Heat and mass transfer in the hollow fiber membrane module is the key issue for performance analysis and system optimization. However, up until now, there are only several feasibility studies [9]. A detailed analysis of heat and mass transfer is still unavailable, not mention an analytical solution.

In this paper, heat and mass transfer in a hollow fiber membrane module is modeled. Further, an analytical solution is obtained for the heat and mass transfer processes. The model can be used conveniently for the estimation of sensible and latent effectiveness. Experiments are conducted to validate the solution. Compared to

* Tel.: +86 20 87114268; fax: +86 20 87114268.
E-mail address: Lzzhang@scut.edu.cn.

0376-7388/$ – see front matter © 2010 Elsevier B.V. All rights reserved.
doi:10.1016/j.memsci.2010.05.015

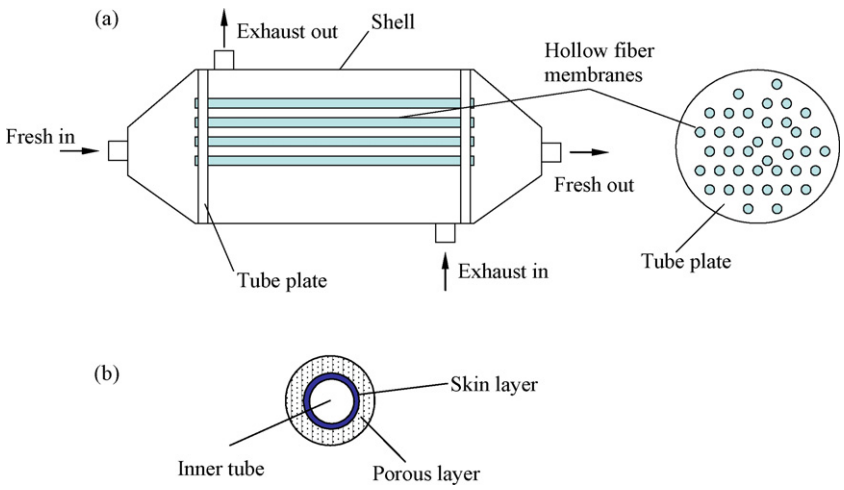

Fig. 1. Schematic representation of the hollow fiber membrane module for heat and moisture recovery. (a) The shell-and-tube structure. (b) Structure of a single membrane fiber.

finite difference iterations, the analytical solution is simple for the engineers to use.

2. Experimental work

2.1. The hollow fiber membrane module

A membrane module is employed to exchange both sensible heat and moisture between the fresh air and the stale exhaust air. The module is like a shell-and-tube heat exchanger, as shown in Fig. 1. The spaces between the shell and the fibers form the shell side flow. Shell side and tube side are separated by the plates. Fresh airflows inside the tubes. Exhaust airflows in the shell side in a counter flow arrangement.

Industrial grade PVDF (polyvinylidene fluoride) supplied by Guangzhou Tianma Co. Ltd. is used as the raw material. The membrane is fabricated by following steps: (1) 15 g PVDF powder is placed in a vessel with 100 g DMF (N,N-dimethylformamide) at about 90 °C. The solution is heated and stirred until the material is completely dissolved. It takes about 2 h. (2) 3 g PEG (polyethylene glycol) and 1 g PVP (polyvinyl pyrrolidone) is added to the solution. It is stirred for another 2 h. (3) The solution is degassed. It is spin into a 25 °C water bath to form fibers. (4) The fibers solidify. They are soaked in water bath for 24 h for solvent and non-solvent exchange. (5) The fiber membranes are dried in a vacuum drying box for 10 h. (6) 5 g modified PVA is dissolved in 100 ml distilled water at 70 °C. The solution is stirred for 5 h. Then the PVA solution is sucked through the inner diameters of the fibers by a pump. The excess solution is blow off the fiber by air stream. A thin layer of PVA is kept on the inner surface of the fibers. They are cross-linked at 70 °C for 10 h. The permselective layer is finally formed inside PVDF fibers. With this step, the defects on the inner surface are also caulked to prevent unwanted gases cross over. The membrane is ready for structural characterization.

In order to observe the morphology of the membranes, the dried membranes are broken in liquid nitrogen. Then the membrane samples are sputtered with a thin layer of gold using a SPI-Module sputter coater. The cross sections are examined using a Joel JSM-5310V scanning microscope (SEM).

Fig. 2 shows the SEM graphs of the cross sections of the fiber. Fig. 2(a) shows the overall structure and Fig. 2(b) shows the details. As seen, it is a typical asymmetric membrane: there are skin layers, the finger-like pores and sponge pores. The porous layers give the necessary mechanical support. The finger-like pores give high permeability.

Then a bundle of 200 fibers are packed in a plastic shell. Tube side and shell side are separated by tube plates. A shell-and-tube structure is formed.

The transport properties in membranes are important. To measure these properties with available test apparatus [14], flat plate

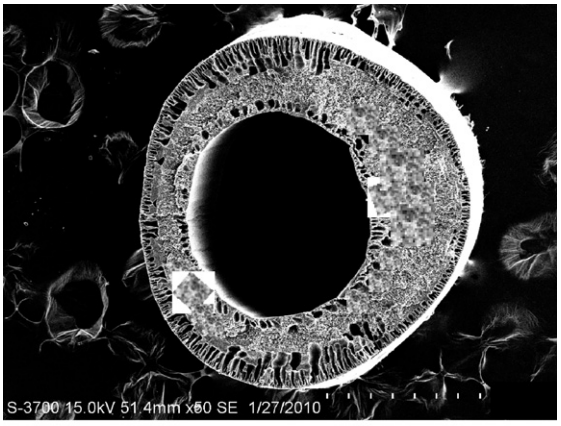

(a) The fiber.

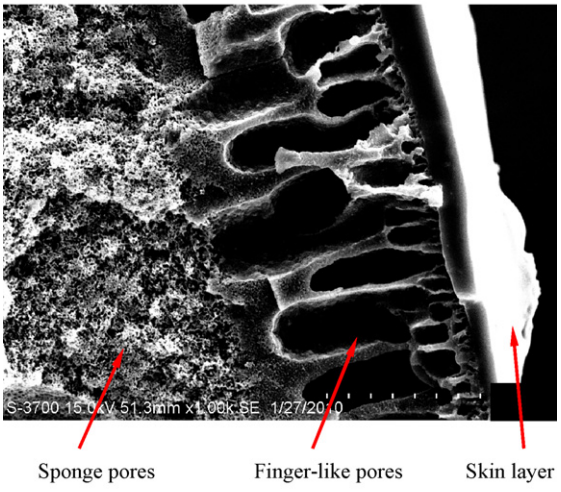

(b) Amplified picture showing the skin layer.

Fig. 2. SEM graphs of the fiber membrane. (a) The fiber. (b) Amplified picture showing the skin layer.

Table 1
Physical and transport properties of the hollow fiber membrane module under design operating conditions.

Name of properties	Symbol	Unit	Values
Shell diameter	D_0	mm	38
Module length	L	mm	300
Number of fibers in the module	n_f		200
Fiber outer diameter	d_o	mm	1.5
Fiber inner diameter	d_i	mm	1.2
Packing fraction	ϕ		0.28
Packing density	A_v	m^2/m^3	750
Moisture diffusivity in air	D_{va}	m^2/s	2.82×10^{-5}
Effective moisture diffusivity in membrane	D_{vm}	m^2/s	3.7×10^{-6}
Heat conductivity of membrane	λ_m	$Wm^{-1}K^{-1}$	0.17
Fresh air temperature	T_{fi}	°C	35.0
Fresh air humidity ratio	ω_{fi}	kg/kg	0.021
Freah air mass flow rate	$\dot{m}_f$	kg/h	5.0
Exhaust air mass flow rate	$\dot{m}_e$	kg/h	5.0
Exhaust air temperature	T_{ei}	°C	25.0
Exhaust air humidity ratio	ω_{ei}	kg/kg	0.009

membranes are also made with above-mentioned raw materials. The ingredients and the making processes are exact the same as those for fiber membranes. However the PVDF membranes are cast on a glass plate before they are put into a water bath. Then PVA solution is coated on the dried plate membranes with a brush. The thickness is estimated by SEM observations. The transport properties (moisture diffusivity, heat conductivity, etc.) are measured and estimated [14]. The obtained data is listed in Table 1. Also listed are the geometrical and the physical properties for the module. The fiber can be considered round, though not exactly round in 50–100 amplified pictures. The deformation is due to being fractured for SEM observations and pressuring in experiments.

2.2. The test rig

An experimental setup has been built to study the simultaneous heat and moisture transport in the hollow fiber membrane module. The whole test rig is shown in Fig. 3. It comprises of an air supply and conditioning unit, a hollow fiber membrane module, and a data acquisition unit.

The whole test rig is in an air-conditioned room. Room air is humidified and driven to a heating/cooling coil in a hot/cool water bath. The cooling coil can be a dehumidifier when necessary. After the temperature and humidity reach set points, the air stream is pumped through the exchanger for experiment. This flow is denoted as the hot and humid fresh stream. Another flow is driven directly from room to the exchanger. It is denoted as the cool and dry exhaust flow. The two flows are arranged in a counter flow configuration, to have maximum exchange effectiveness, as shown in Fig. 4. In the test, a 10-mm thick insulation layer is placed on the outer surface of the shell to prevent heat dissipation from the shell

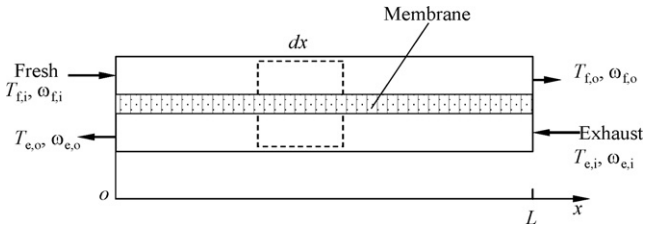

Fig. 4. Heat and moisture transfer model in the hollow fiber membrane module.

to the surroundings. Moisture dissipation from air stream to the surroundings is negligible. After the exchanger and pipes are connected together, additional insulation is added on the tubes and exchangers to minimize heat losses from the test rig. The humidity and temperature of the exhaust air can be adjusted by adjusting room air states.

The nominal operating conditions are: fresh air inlet 35 °C and 0.021 kg/kg; exhaust air inlet 25 °C and 0.010 kg/kg. The corresponding inlet relative humidity (*RH*) is 59% and 51% for fresh air and exhaust air respectively. The designed conditions for airflow rates are 5 kg/h with balanced flow. During the experiment, airflow rate can be changed by variable frequency pumps to have different air velocities. Humidity, temperature, and volumetric flow rates are monitored at the inlet and outlet of the exchanger. In air ventilation, it is normal to have balanced flows. However to validate the model, unbalanced flows are sometimes conducted. Volumetric airflow rates are varied from 4.2 kg/h to 7.2 kg/h, corresponding to air velocities from 1 m/s to 4 m/s. Airflow under such conditions is laminar, with Reynolds numbers not exceeding 500. The uncertainties are: temperature ±0.1 °C; humidity ±2%; volumetric flow rate ±1%. The final uncertainty for effectiveness is ±4.5%. The uncertainties of sensors are defined by the manufacturers. The uncertainties for the deduced value are estimated by uncertainty transfer equations, as introduced in Ref. [15].

3. The mathematical model

3.1. Overall heat mass transfer coefficients from solution to air stream

3.1.1. Pressure drop and convective heat mass transfer coefficients

Reynolds number is defined by

$$Re = \frac{d_h u}{\nu} \tag{1}$$

$$\Delta P = f \cdot L \cdot \frac{\rho_a}{2} \frac{u^2}{d_h} \tag{2}$$

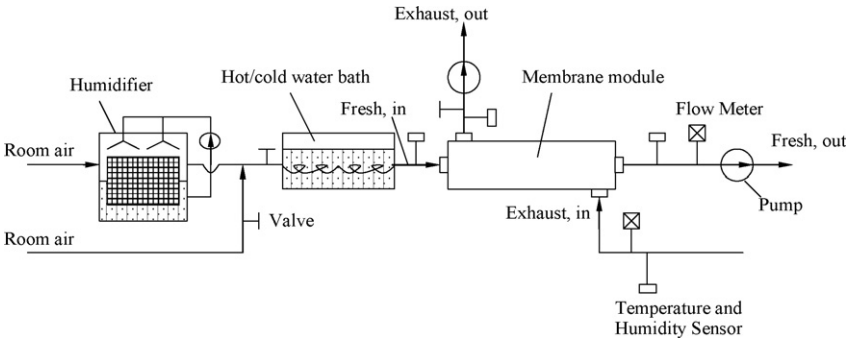

Fig. 3. The experimental setup for membrane module heat and moi sture recovery.

where in the equations, Re is Reynolds number; d_h is the hydrodynamic diameter (m). For tube, it is d_i, for shell side, it should be calculated. Other variables are: u is air mean velocity (m/s); ν is air viscosity (m^2/s); ΔP is pressure drop (Pa); f is friction factor; L is module length (m); ρ_a is air density (kg/m^3). For tube side, the air is fresh air (subscript "f"), and for shell side, the air is exhaust air (subscript "e").

Convective mass transfer coefficient k (m/s) and heat transfer coefficient h ($kW\,m^{-2}\,K^{-1}$) can be represented by Sherwood and Nusselt numbers respectively as

$$Sh = \frac{kd_h}{D_{va}} \tag{3}$$

$$Nu = \frac{hd_h}{\lambda} \tag{4}$$

where according to Chilton–Colburn analogy [11]

$$Nu = Sh \cdot Le^{1/3} \tag{5}$$

where

$$Le = \frac{Pr}{Sc} \tag{6}$$

$$Pr = \frac{\nu}{\alpha} \tag{7}$$

$$Sc = \frac{\nu}{D_{va}} \tag{8}$$

where D_{va} represents moisture diffusivity in air; Le is the Lewis number of air; Pr, and Sc are Prandtl number and Schmidt number respectively, α is thermal diffusivity for air (m^2/s).

3.1.2. Tube side correlations

Fresh airflows in tube side. For laminar flow in round tubes, the product of friction factor and Reynolds number satisfies [16]

$$(f \cdot Re) = 64 \tag{9}$$

Mass transfer inside hollow fiber membranes is governed by [17–19]

$$Sh = 1.62\left(\frac{d_i^2 u_i^2}{LD_{va}}\right)^{1/3} \tag{10}$$

3.1.3. Shell side correlations

Exhaust airflows in shell side. Established correlation for mass transfer in shell side of a hollow fiber membranes module is [18]

$$Sh = (0.53 - 0.58\phi)Re^{0.53}Sc^{0.33} \tag{11}$$

where ϕ is the packing fraction of the module, which is the ratio of total cross-sectional area of the fibers to the module.

$$\phi = \frac{n_f d_o^2}{D_0^2} \tag{12}$$

where D_0 is the diameter of the module shell (m); d_o is the outer diameter of a single fiber (m); n_f is the number of fibers in the module. In practice, diameters and thickness of each fiber may be somewhat different, the mean values are used.

The airflow area in shell side

$$A_{flow} = (1 - \phi)\frac{\pi D_0^2}{4} \tag{13}$$

The hydrodynamic diameter in shell side is defined to 4 times of flow area divided by total perimeter of membrane fibers

$$d_h = \frac{4A_{flow}}{n_f \pi d_o} = \frac{(1 - \phi)D_0^2}{n_f d_o} \tag{14}$$

The packing density A_v (m^2/m^3) is the ratio of total membrane area to module volume

$$A_v = \frac{4n_f d_o}{D_0^2} \tag{15}$$

Resistance through the shell side is measured. It is related to packing density and flow configurations. A correlation can be summarized to estimate the product of friction factor and Reynolds number as

$$(f \cdot Re) = 41.3 \tag{16}$$

3.1.4. Overall heat and mass transfer coefficients

Resistances from fresh air to exhaust air can be considered as a sum of resistances in series. The overall mass and heat transfer coefficients from fresh to exhaust air on the basis of outer surface of the fibers are calculated by [17–19]

$$\frac{1}{k_{tot}} = \frac{1}{k_i}\left(\frac{d_o}{d_i}\right) + \frac{\delta}{D_{vm}}\left(\frac{d_o}{\bar{d}}\right) + \frac{1}{k_o} \tag{17}$$

$$\frac{1}{h_{tot}} = \frac{1}{h_i}\left(\frac{d_o}{d_i}\right) + \frac{\delta}{\lambda_m}\left(\frac{d_o}{\bar{d}}\right) + \frac{1}{h_o} \tag{18}$$

where $\bar{d}$ is the arithmetic mean diameter of a fiber, i.e., $(0.5^*(d_o + d_i))$; D_{vm} is the effective moisture diffusivity in membranes (m^2/s), which is measured in the laboratory by FLEC system [14]; δ is membrane thickness (m).

3.2. Module effectiveness

Sensible and latent (moisture) effectiveness of the module is defined by

$$\varepsilon_{sen} = \frac{\dot{m}_f c_{pf}(T_{fi} - T_{fo})}{(\dot{m}c_p)_{min}(T_{fi} - T_{ei})} = \frac{\dot{m}_e c_{pe}(T_{eo} - T_{ei})}{(\dot{m}c_p)_{min}(T_{fi} - T_{ei})} \tag{19}$$

$$\varepsilon_{Lat} = \frac{\dot{m}_f(\omega_{fi} - \omega_{fo})}{(\dot{m})_{min}(\omega_{fi} - \omega_{ei})} = \frac{\dot{m}_e(\omega_{eo} - \omega_{ei})}{(\dot{m})_{min}(\omega_{fi} - \omega_{ei})} \tag{20}$$

where T is temperature (K), subscripts "i" and "o" here mean inlet and outlet respectively; $\dot{m}$ is the total mass flow rate of dry air of fresh air (subscript f) or exhaust air (subscript e) (kg/s); Subscript "min" refers to the fluid with the lower heat or mass capacity between the two streams.

Heat and mass capacity ratios of the two fluids are defined by

$$C_{sen} = \frac{(\dot{m}c_p)_{min}}{(\dot{m}c_p)_{max}} \tag{21}$$

and

$$C_{Lat} = \frac{(\dot{m})_{min}}{(\dot{m})_{max}} \tag{22}$$

3.3. Heat and mass conservation equations

A mesoscopic scale model is set up. For the hollow fiber membrane module, a control volume in fresh airflow direction is shown in Fig. 4. The two air streams flow in a counter flow arrangement, while exchanging heat and moisture through membranes.

Following assumptions are made:

(1) The problem is one dimensional.
(2) Heat and moisture losses through the shell to the surroundings are neglected.
(3) Axial dispersion of heat and mass are neglected.
(4) Constant physical properties.
(5) Adsorption heat in fresh air side is balanced by desorption heat in exhaust side.

The diffusion mechanism of moisture through the membranes has been explained in Ref. [11]. Solution-diffusion was considered for membrane resistance. In this study, the flows are in counter flow arrangements. The trans-membrane temperature and humidity differences across the membrane are small. When the operating conditions across the membrane are similar, the diffusivity across the membrane can be assumed a constant, at least during the narrow operating conditions. In Ref. [11], the diffusivity is estimated by the relations between the membrane material and operating conditions. In this study, the value of diffusivity is experimentally obtained in advance, under the same operating conditions as hollow fiber modules. Finding an analytical solution would be difficult, if the diffusivity is not assumed a constant. This is a reasonable assumption.

Besides, in air conditioning operating conditions, water vapor usually accounts for less than 2% of weight in air. The contribution of vapor sensible heat to the total air sensible heat is negligible.

Heat and moisture conservation in the fresh air stream are

$$\dot{m}_f c_{pf} \frac{dT_f}{dx} = \frac{h_{tot} A_{tot}}{L}(T_e - T_f) \tag{23}$$

$$\dot{m}_f \frac{d\omega_f}{dx} = \frac{\rho_a k_{tot} A_{tot}}{L}(\omega_e - \omega_f) \tag{24}$$

where in the equations, A_{tot} is the total area of the outer surface of fibers (m^2).

Heat and moisture conservation in the exhaust air stream are

$$\dot{m}_e c_{pe} \frac{dT_e}{dx} = \frac{h_{tot} A_{tot}}{L}(T_e - T_f) \tag{25}$$

$$\dot{m}_e \frac{d\omega_e}{dx} = \frac{\rho_a k_{tot} A_{tot}}{L}(\omega_e - \omega_f) \tag{26}$$

To simplify the equations, dimensionless temperature and humidity are defined by

$$T^* = \frac{T - T_{ei}}{T_{fi} - T_{ei}} \tag{27}$$

$$\omega^* = \frac{\omega - \omega_{ei}}{\omega_{fi} - \omega_{ei}} \tag{28}$$

$$x^* = \frac{x}{L} \tag{29}$$

As seen, at fresh air inlet (or exhaust air outlet) where $x^* = 0$

$$T^*_{fi} = 1 \tag{30}$$

$$\omega^*_{fi} = 1 \tag{31}$$

At fresh air outlet (or exhaust air inlet) where $x^* = 1$

$$T^*_{ei} = 0 \tag{32}$$

$$\omega^*_{ei} = 0 \tag{33}$$

Substituting Eqs. (27)–(29) into Eqs. (23) and (24), normalized equations for heat and moisture conservation in fresh air are

$$\frac{dT^*_f}{dx^*} = NTU_{sen,f}(T^*_e - T^*_f) \tag{34}$$

$$\frac{d\omega^*_f}{dx^*} = NTU_{Lat,f}(\omega^*_e - \omega^*_f) \tag{35}$$

where

$$NTU_{sen,f} = \frac{h_{tot} A_{tot}}{(\dot{m} c_p)_f} \tag{36}$$

$$NTU_{Lat,f} = \frac{\rho_a k_{tot} A_{tot}}{(\dot{m})_f} \tag{37}$$

$$Le_{tot} = \frac{NTU_{sen}}{NTU_{Lat}} = \frac{h_{tot}}{\rho_a c_p k_{tot}} \tag{38}$$

where Le_{tot} is called the overall Lewis number, which reflects the ratio of overall heat transfer coefficient to overall mass transfer coefficient. For membrane systems, mass transfer resistance is usually larger than heat transfer resistance, therefore the overall Lewis number is always greater than unity.

Similarly, substituting Eqs. (27)–(29) into Eqs. (25) and (26), normalized equations for heat and moisture conservation in exhaust air are

$$\frac{dT^*_e}{dx^*} = NTU_{sen,e}(T^*_e - T^*_f) \tag{39}$$

$$\frac{d\omega^*_e}{dx^*} = NTU_{Lat,e}(\omega^*_e - \omega^*_f) \tag{40}$$

where

$$NTU_{sen,e} = \frac{h_{tot} A_{tot}}{(\dot{m} c_p)_e} \tag{41}$$

$$NTU_{Lat,e} = \frac{\rho_a k_{tot} A_{tot}}{(\dot{m})_e} \tag{42}$$

3.4. Analytical solutions

Eqs. (34), (35) and (39), (40) are the governing differential equations for heat and moisture transfer in the module. They can be solved by finite difference iterations, with known heat mass transport properties. However they are difficult for common engineers to use. In contrast, analytical solutions for above differential equations will be convenient and helpful for common designers to use.

Subtracting Eq. (34) with (39), we have

$$\frac{d(T^*_f - T^*_e)}{dx^*} = -NTU_{sen}(1 - C_{sen})(T^*_f - T^*_e) \tag{43}$$

Subtracting Eq. (35) with (40), we have

$$\frac{d(\omega^*_f - \omega^*_e)}{dx^*} = -NTU_{Lat}(1 - C_{Lat})(\omega^*_f - \omega^*_e) \tag{44}$$

where the Number of Transfer Units for the whole module are

$$NTU_{sen} = \frac{h_{tot} A_{tot}}{(\dot{m} c_p)_{min}} \tag{45}$$

$$NTU_{Lat} = \frac{\rho_a k_{tot} A_{tot}}{(\dot{m})_{min}} \tag{46}$$

Eqs. (43) and (44) can be transformed to

$$\frac{d(T^*_f - T^*_e)}{(T^*_f - T^*_e)} = -NTU_{sen}(1 - C_{sen})\, dx^* \tag{47}$$

$$\frac{d(\omega^*_f - \omega^*_e)}{(\omega^*_f - \omega^*_e)} = -NTU_{Lat}(1 - C_{Lat})\, dx^* \tag{48}$$

Integration of Eq. (47) from $x^* = 0$ to 1, we have

$$\frac{(T^*_f - T^*_e)_{x^*=1}}{(T^*_f - T^*_e)_{x^*=0}} = \exp\left[-NTU_{sen}(1 - C_{sen})\right] \tag{49}$$

or

$$\frac{T^*_{fo}}{1 - T^*_{eo}} = \exp\left[-NTU_{sen}(1 - C_{sen})\right] \tag{50}$$

Assuming the fresh air has the minimum heat capacity, then substituting Eqs. (27), (30), (32) into (19) and (21), we will have

$$\varepsilon_{sen} = 1 - T^*_{fo} \tag{51}$$

$$C_{sen} = \frac{T^*_{eo}}{1\text{-}T^*_{fo}} \tag{52}$$

Table 2
Operating conditions for the hollow fiber membrane module.

Exp. no.	Operating conditions					
	Fresh air			Exhaust air		
	$\dot{m}_f$ (kg/h)	T_{fi} (°C)	ω_{fi} (kg/kg)	$\dot{m}_e$ (kg/h)	T_{ei} (°C)	ω_{ei} (kg/kg)
A	5.2	34.8	0.021	5.6	25.1	0.009
B	5.2	33.9	0.018	5.0	24.9	0.008
C	4.8	35.2	0.022	5.4	25.3	0.008
D	4.2	34.9	0.021	6.3	25.2	0.010
E	7.2	33.7	0.019	5.5	25.2	0.008
F	5.1	33.8	0.021	4.9	25.5	0.007
G	5.3	35.3	0.022	5.1	24.5	0.010
H	5.1	32.8	0.019	4.7	24.6	0.009
I	4.8	29.8	0.018	5.6	24.6	0.008
J	6.5	27.2	0.016	6.6	25.6	0.007
K	5.8	28.7	0.014	5.7	25.1	0.010

Substituting Eqs. (51) and (52) into (50), the solution will give the analytical expression for sensible effectiveness

$$\varepsilon_{sen} = \frac{1 - \exp[-NTU_{sen}(1 - C_{sen})]}{1 - C_{sen}\exp[-NTU_{sen}(1 - C_{sen})]} \quad (53)$$

As seen, the expression is in accordance with the ε-NTU correlations for a counter flow heat exchanger [16]. Similarly, when $C_{sen} = 1$, the expression becomes

$$\varepsilon_{sen} = \frac{NTU_{sen}}{1 + NTU_{sen}} \quad (54)$$

For mass transfer, Eq. (48) is in the same form with Eq. (47). This is called the heat mass transfer analogy. With the same method of solution as for Eq. (45), the latent effectiveness can be solved as

$$\varepsilon_{Lat} = \frac{1 - \exp[-NTU_{Lat}(1 - C_{Lat})]}{1 - C_{Lat}\exp[-NTU_{Lat}(1 - C_{Lat})]} \quad (55)$$

When $C_{Lat} = 1$, the expression becomes

$$\varepsilon_{Lat} = \frac{NTU_{Lat}}{1 + NTU_{Lat}} \quad (56)$$

When the effectiveness is calculated, the outlet conditions can be calculated then.

4. Results and discussion

4.1. Model validation

Experimental work is used to validate the model and the methodology. Under normal operating conditions, the airflow rates, and temperature and humidity are changed to have different flow conditions. Eleven tests, from Exp. A to K, are used to represent the sample tests. All of them realized steady state balances. The inlet conditions are listed in Table 2.

The measured outlet temperature and humidity for the two streams are listed in Table 3. The outlet parameters for the two streams are also calculated by finite difference model (FD) and the analytical solution (ANL). The finite difference is calculated by Eqs. (23)–(26), and the analytical model is calculated by Eqs. (53)–(56). The three results are compared. If we know the analytical solution "has already been" the right solution, there is no need to use finite difference anymore. The analytical solutions can be seen as the solutions for finite difference model with infinite number of nodes. When the number of nodes is large enough, the two solutions are the same. This method is used to validate the analytical solutions with finite difference model, or vice versa. After the validation, in future we can use the exact solutions directly, without finite difference models.

As can be seen, the numerical results fit the experiments well. The differences between the analytical solution and the finite difference model are less than 0.2% for temperature and 9% for humidity, respectively. The analytical model predicts the test rather satisfactorily. The maximum difference for temperature is below 3%, and the maximum difference for humidity is below 10%. The humidity has larger discrepancies due to the larger uncertainties in humidity measurements. Generally, the measured data and the calculated data agree well, meaning the model and the analytical solution are successful in modeling heat and mass transfer problems in hollow fiber membrane based air-to-air heat mass exchanger.

Table 3
Comparisons of outlet conditions obtained from finite difference calculation, analytical solution, and the test results.

Exp. no.	Fresh air						Exhaust air					
	T_{fo} (°C)			ω_{fo} (kg/kg)			T_{eo} (°C)			ω_{eo} (kg/kg)		
	FD	ANL	Test	FD	ANL	Test	FD	ANL	Test	FD	ANL	Test
A	27.0	27.1	27.5	0.013	0.012	0.011	32.6	32.8	32.5	0.016	0.017	0.018
B	26.5	26.6	27.0	0.012	0.011	0.012	32.3	32.5	32.1	0.015	0.016	0.017
C	27.3	27.5	27.1	0.010	0.011	0.012	33.1	33.0	33.2	0.017	0.018	0.019
D	28.9	28.8	29.2	0.011	0.012	0.013	31.2	31.3	31.6	0.017	0.016	0.017
E	27.6	27.8	27.5	0.013	0.012	0.011	32.8	32.9	33.1	0.016	0.017	0.016
F	27.0	27.1	28.0	0.010	0.011	0.012	32.6	32.5	33.1	0.019	0.018	0.018
G	26.6	26.5	26.9	0.012	0.013	0.013	33.5	33.6	33.2	0.018	0.019	0.018
H	26.5	26.3	26.0	0.012	0.012	0.011	31.6	31.7	32.2	0.017	0.017	0.016
I	25.8	25.9	25.6	0.011	0.010	0.011	28.6	28.5	29.1	0.012	0.013	0.014
J	25.7	25.9	25.3	0.012	0.010	0.011	26.8	26.9	26.3	0.014	0.013	0.012
K	25.6	25.8	25.2	0.010	0.011	0.012	28.3	28.1	28.6	0.012	0.012	0.011

Notes: FD, finite difference; ANL, analytical solution.

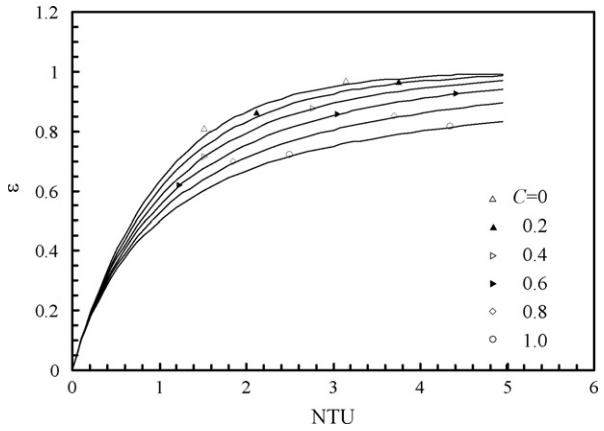

Fig. 5. Effects of *NTU* and *C* on effectiveness for a counter flow module.

4.2. Application of the model

As seen from Eqs. (53)–(56), the operating and design conditions can be summarized in the non-dimensional parameters of *NTU* and *C*. Subscript "sen" is for sensible and "Lat" is for latent heat exchange. The sensible and latent effectiveness is solely determined by these two dimensionless parameters. The effects of *NTU* and *C* on the effectiveness are calculated with Eqs. (53) and (56). They are drawn in Fig. 5. As seen, the higher the *NTU*, the greater the effectiveness. The *NTU* has greater influences when it is from 0 to 3. When *NTU* is greater than 3, its effects become less. Therefore too many fibers will have no greater benefits in further enhancing performances. The optimum *NTU* should be near 3–4.

The less the *C* is, the higher the effectiveness is. When $C = 1$, or for the balanced flow, the effectiveness is the least. In ventilation, balanced flow is common.

The pressure drop balance between shell-and-tube sides should be considered for hollow fiber modules. When the geometries are correctly designed, the balanced flow can be ensured. This paper is just to provide a tool for performance design and optimization. Everything has merits and demerits, how to use merits and overcome demerits are the key to success. For this study, the effectiveness and pressure drop correlations would help to overcome these pressure penalties, by properly controlling packing density and fiber diameter.

Above analysis is classical for a sensible-only heat exchanger. However from this analysis, it is found that the same rules also hold for mass exchange. The established correlations provide a simple design tool for hollow fiber membrane module, which are more complicated due to complex structure and simultaneous heat mass exchange.

By setting other parameters unchanged under the design operating conditions, the effects of the number of fibers in the module are discussed. Fig. 6 shows its effects on NTU_{sen} and NTU_{Lat}, and on the consequent sensible and latent effectiveness. The inner diameter of the fiber is fixed to 1.2 mm. The number of the fiber, n_f, influences the exchange area directly. As seen, when n_f is increased from 50 to 250, the NTU_{sen} increases from 1.06 to 5.93, while the NTU_{Lat} increases from 0.64 to 3.4. Correspondingly, the sensible effectiveness increases from 0.52 to 0.86, while the latent effectiveness increases from 0.39 to 0.77. The step of increase becomes slower when n_f is larger than 150.

On the other hand, the value of NTU_{Lat} is generally less than that of NTU_{sen}. When the n_f is increased from 50 to 250, the overall Lewis number ($Le_{tot} = Nu_{sen}/Nu_{Lat}$) varies from 0.60 to 0.57. The variations are relatively small.

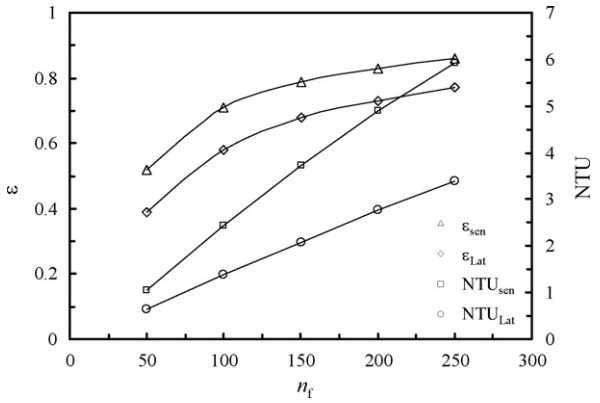

Fig. 6. Effects of the number of fibers on performance, $d_i = 1.2$ mm.

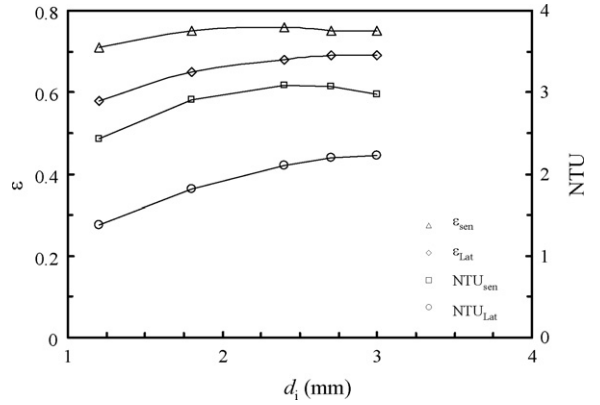

Fig. 7. Effects of fiber diameter on performance, $n_f = 100$.

Fig. 7 shows the effects of the inner diameter of the fibers, d_i, on performances. The number of the fibers is fixed to 100. As seen, when the d_i is increased from 1.2 mm to 3.0 mm, the NTU_{sen} increases from 2.43 to 2.98. At the same time, the NTU_{Lat} increases form 1.38 to 2.23. The increases in *NTU* are mainly due to the increased contact area. However the variations are not large. Correspondingly, the sensible effectiveness changes little at 0.75. The latent effectiveness keeps to 0.68. Therefore the fiber diameter has little influence on performances. However, it has a great impact on pressure drops. As seen from Fig. 8, the larger the fiber diameters are, the less the tube side pressure drops are, and the greater the shell side pressure drops are. They are explained by the following.

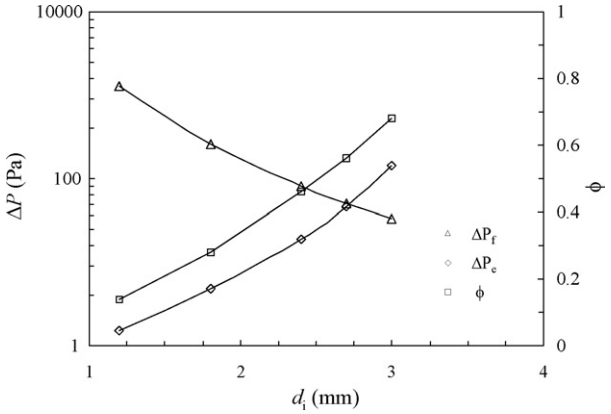

Fig. 8. Effects of fiber diameter on pressure drops.

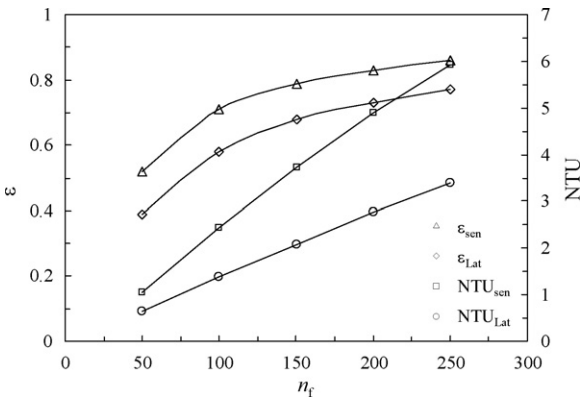

Fig. 9. Profiles of dimensionless temperature and humidity along axial direction.

The larger the fiber diameters are, the larger the tube side spaces are, and the less the shell side spaces are. The packing fraction is increased from 0.14 to 0.56 when the fiber diameter is increased from 1.2 mm to 3 mm. For heat and moisture recovery, it is better to have a balanced pressure drop, so a 2.7-mm diameter is the optimum one. In such cases, the tube and shell sides have equal pressure drops.

The effectiveness and the outlet parameters can be calculated easily with the established correlations. However they are unable to disclose the parameters inside the module. The parameters inside will be helpful to know the heat mass transfer mechanisms in the module. In this section, the temperature and humidity along the module length are calculated with the finite difference model. The dimensionless temperature and humidity are plotted in Fig. 9. As seen, the fresh air temperature and humidity decrease along the flow. The step of decrease in humidity is slower than that in temperature, meaning high mass transfer resistance. In contrast, the exhaust air temperature and humidity increase along counter x direction.

5. Conclusions

Heat and mass transfer in a hollow fiber membrane module which is used for air-to-air heat mass exchanger are studied. The heat and mass transfer model from the fresh air to the exhaust air stream is set up. An analytical solution is obtained to estimate the sensible and moisture effectiveness. Some results can be found:

(1) Comprised of solely algebraic correlations, the obtained analytical model is accurate and convenient for the estimation of sensible and latent effectiveness for a counter flow heat mass exchanger.
(2) The Number of Transfer Units (*NTU*) and capacity ratio *C* are the determining factors influencing performances. The established correlations, which are classical for sensible-only heat exchangers, can be extended to heat mass exchanger analysis.
(3) The number of fibers, fiber diameters, and other operating conditions can be optimized with the established correlations. More specifically for this study, the optimum fiber diameter is 2.7 mm; and the optimized number of fibers is 150. A module with these parameters will have a sensible effectiveness above 0.7 and a latent effectiveness above 0.6.

Acknowledgements

The Project is supported by National Natural Science Foundation of China, No. 50676034, and The Fundamental Research Funds for the Central Universities, 2009ZZ0060.

Nomenclature

A	area (m^2)
A_v	packing density (m^2/m^3)
c_p	specific heat of air ($kJ\,kg^{-1}\,K^{-1}$)
C	dimensionless heat or mass capacity ratio
D	diffusivity (m^2/s)
d	diameter (m)
$\bar{d}$	arithmetic mean diameter (m)
D_0	Shell diameter (m)
d_h	hydrodynamic diameter (m)
f	friction factor
h	convective heat transfer coefficient ($kW\,m^{-2}\,K^{-1}$)
k	convective mass transfer coefficient (m/s)
L	length (m)
Le	Lewis number
$\dot{m}$	mass flow rate (kg/s)
n_f	number of fibers
NTU	Number of Transfer Units
Nu	Nusselt number
P	pressure (Pa)
p_v	vapor pressure (Pa)
Pr	Prandtl number
Re	Reynolds number
Sc	Schmidt number
Sh	Sherwood number
T	temperature (K)
u	velocity (m/s)
x	axial coordinate (m)

Greek letters

ε	effectiveness
ϕ	packing fraction
α	thermal diffusivity (m^2/s)
ρ	density (kg/m^3)
λ	heat conductivity ($W\,m^{-1}\,K^{-1}$)
ω	humidity ratio (kg/kg)
ν	kinematic viscosity (m^2/s)
δ	membrane thickness (m)

Superscript

*	dimensionless

Subscripts

a	air
f	fresh air, fiber
e	exhaust air
i	inlet, inner
Lat	moisture, latent
m	mean, membrane, mass
o	outlet, outer
sen	sensible
tot	total
v	vapor

References

[1] Y.P. Zhang, R. Yang, R.Y. Zhao, A model for analyzing the performance of photocatalytic air cleaner in removing volatile organic compounds, Atmospheric Environment 37 (2003) 3395–3399.
[2] J.H. Mo, Y.P. Zhang, R. Yang, Novel insight into VOC removal performance of photocatalytic oxidation reactors, Indoor Air 15 (2005) 291–300.
[3] Y. Xu, Y.P. Zhang, An improved mass transfer based model for analyzing VOC emissions from building materials, Atmospheric Environment 37 (2003) 2497–2505.

[4] Y. Xu, Y.P. Zhang, A general model for analyzing VOC emission characteristics from building materials and its application, Atmospheric Environment 38 (2004) 113–119.
[5] X.H. Liu, Y. Zhang, K.Y. Qu, Y. Jiang, Experimental study on mass transfer performances of cross flow dehumidifier using liquid desiccant, Energy Conversion and Management 47 (2006) 2682–2692.
[6] X.H. Liu, Z. Li, Y. Jiang, B.R. Lin, Annual performance of liquid desiccant based independent humidity control HVAC system, Applied Thermal Engineering 26 (2006) 1198–1207.
[7] L.Z. Zhang, Total Heat Recovery: Heat and Moisture Recovery from Ventilation Air, Nova Science Publishing Co., New York, 2008, p. 14 (Chapter 1).
[8] L.Z. Zhang, J.L. Niu, Energy requirements for conditioning fresh air and the long-term savings with a membrane-based energy recovery ventilator in Hong Kong, Energy 26 (2) (2001) 119–135.
[9] K.R. Kistler, E.L. Cussler, Membrane modules for building ventilation, Chemical Engineering Research and Design 80 (2002) 53–64.
[10] L.Z. Zhang, J.L. Niu, Effectiveness correlations for heat and moisture transfer processes in an enthalpy exchanger with membrane cores, ASME Journal of Heat Transfer 124 (2002) 922–929.
[11] J.L. Niu, L.Z. Zhang, Membrane-based enthalpy exchanger: material considerations and clarification of moisture resistance, Journal of Membrane Science 189 (2001) 179–191.
[12] J.C. Min, M. Su, Performance analysis of a membrane-based enthalpy exchanger: effects of the membrane properties on the exchanger performance, Journal of Membrane Science 348 (2010) 376–382.
[13] T. Hu, J.C. Min, Y.Z. Song, Modeling and analysis of dynamic adsorption during gas transport through a membrane, Journal of Membrane Science 339 (2009) 204–208.
[14] L.Z. Zhang, Y.Y. Wang, C.L. Wang, H. Xiang, Synthesis and characterization of a PVA/LiCl blend membrane for air dehumidification, Journal of Membrane Science 308 (2008) 198–206.
[15] X.H. Liu, Y. Jiang, K.Y. Qu, Analytical solution of combined heat and mass transfer performance in a cross-flow packed bed liquid desiccant air dehumidifier, International Journal of Heat and Mass Transfer 51 (2008) 4563–4572.
[16] F.P. Incropera, D.P. Dewitt, Introduction to Heat Transfer, 3rd ed., John Wiley & Sons, New York, 1996, p. 416 (Chapter 8).
[17] S. Atchariyawut, C. Feng, R. Wang, R. Jiraratananon, D.T. Liang, Effect of membrane structure on mass transfer in the membrane gas–liquid contacting process using microporous PVDF hollow fibers, Journal of Membrane Science 285 (2006) 272–281.
[18] M.J. Costello, A.G. Fane, P.A. Hogan, R.W. Schofield, The effect of shell side hydrodynamics on the performance of axial flow hollow fiber modules, Journal of Membrane Science 80 (1993) 1–11.
[19] R.M.C. Viegas, M. Rodriguez, S. Luque, J.R. Alvarez, I.M. Coelhoso, J.P.S.G. Crespo, Mass transfer correlations in membrane extraction: analysis of Wilson-plot methodology, Journal of Membrane Science 245 (1998) 129–142.